Biosensors and Bioelectronics 26 (2010) 615–619

Contents lists available at ScienceDirect

Biosensors and Bioelectronics

journal homepage: www.elsevier.com/locate/bios

Label-free optical biosensor based on localized surface plasmon resonance of twin-linked gold nanoparticles electrodeposited on ITO glass

Jiajia Deng, Yan Song, Yuan Wang, Junwei Di*

College of Chemistry, Chemical Engineering and Material Science, Soochow University, Suzhou, Jiangsu 215123, PR China

ARTICLE INFO

Article history:
Received 4 April 2010
Received in revised form 4 July 2010
Accepted 6 July 2010
Available online 14 July 2010

Keywords:
Localized surface plasmon resonance
Label-free
Twin-linked gold nanoparticles
Biosensor

ABSTRACT

A simple low-cost electrochemical approach has been used to directly deposit twin-linked gold nanoparticles (TGNPs) onto transparent indium tin oxide (ITO) coated film glass. The as-prepared TGNPs have a transverse localized surface plasmon resonance (LSPR) band at 540 nm and a longitudinal LSPR band at about 710 nm. The longitudinal LSPR band of TGNPs exhibits higher refractive index sensitivity (245 nm/RIU) than its transverse LSPR band. The resulting "clean" surface of the TGNPs is easy applied to the further modification. The subsequent bioconjugation of TGNP films with goat anti-mouse-immunoglobulin G (anti-m-IgG) is successfully employed for the detection of mouse-immunoglobulin G (m-IgG) in a model based on the specific binding affinity between the antigen and antibody. The spectrophotometric sensor shows concentration-dependent binding for m-IgG. This study reveals a simple and sensitive method to fabricate a label-free optical biosensor based on longitudinal LSPR band of TGNPs on ITO substrate.

1. Introduction

Gold nanoparticles (GNPs) exhibit localized surface plasmon resonance (LSPR) at visible and near-infrared frequencies, leading to sharp peaks in their spectral extinction. The LSPR wavelength and intensity depends on the size, shape, and dielectric properties of the nanostructure, as well as on its dielectric environment and the presence of nearby nanostructure. The LSPR spectral extinction peak is sensitive to the surrounding media's refractive index, which allows LSPR-active nanostructures to act as transducers in label-free biosensors. That is, by observing spectral shifts in the LSPR wavelength, one can directly measure molecular binding to a nanoparticle surface through minute changes in the particle's dielectric environment (Stewart et al., 2008; Sepúlveda et al., 2009). LSPR sensing is analogue of the nanoparticle surface plasmon resonance (SPR) sensing with a thin gold film. Recently, LSPR based nanosensors have been developed to complement of the SPR sensors. Furthermore, since LSPR sensing is based on a simple optical extinction measurement, it can be minimized to a small spatial element and is not temperature sensitive. The major advantages of LSPR sensing over convention SPR are the simple experimental setup and lower cost because the experiments can be reduced to measurements at a single wavelength in a transmission configuration at a UV–vis spectrophotometer (Shon et al., 2009; Haes and Van Duyne, 2004; Beeram and Zamborini, 2009).

GNPs are widely used for fabrication of biosensor because their surface can be easily and efficiently modified. Moreover, the biosafety and biocompatibility of GNPs is well established (Connor et al., 2005; Wang and Ma, 2009). Nath and Chilkoti reported the label-free optical biosensor based on LSPR of gold nanospheres (Nath and Chilkoti, 2002, 2004). It was reported that the Au nanospheres at a diameter about 35 nm showed an absorption band around 530 nm and low refractive index sensitivity (45 nm/RIU, refractive index unit). With the increasing the diameter of GNPs, the LSPR band was red-shifting and the refractive index sensitivity was increasing. The refractive index sensitivity reached 187 nm/RIU at the about 130 nm of GNPs with LSPR band at approximately 600 nm (Wang et al., 2009). Nonspherical nanostructures offer the possibility of tuning the optical properties over a broad spectral range. For example, LSPR of gold nanorods are one of the most widely studied topics in the field of nanoparticle optical properties and biosensors (Huang et al., 2009c; Chen et al., 2007; Yang and Cui, 2008). Gold nanorods exhibit two LSPR bands in the vis–NIR spectral range. The band near 530 nm has been assigned to a transverse LSPR, which is polarized across (corresponding to electron oscillation perpendicular to) the long axis of the nanorod, and the other one, appearing at a longer wavelength, has been assigned to a longitudinal LSPR mode, which is polarized along (parallel to) the long axis. The longitudinal LSPR band is highly sensitive to the change in the refractive index of the environment, and the refractive index sensitivity is much higher than that of Au nanospheres.

* Corresponding author. Tel.: +86 51265880354; fax: +86 512 65880089.
E-mail address: djw@suda.edu.cn (J. Di).

0956-5663/$ – see front matter © 2010 Elsevier B.V. All rights reserved.
doi:10.1016/j.bios.2010.07.014

However, one critical obstacle against the gold nanorod exploration in the field of biosensing is the use of cetyltrimethylammonium bromide (CTAB), which functions not only as rod-shape inducing agents, but also as capping agents (Pérez-Juste et al., 2005). The presence of surfactant molecules on the surface of the nanorods strongly influences their reactivity and stability. The CTAB molecules are commonly hard to be displaced by or incorporated with biomolecules of interest. For further biological applications, excessive CTAB should be removed, which can be achieved by repeatedly centrifuging the gold nanorod solution. However, CTAB molecules on the gold nanorod surface can only be removed partially because the obtained gold nanorods are not stable mainly due to desorption of CTAB molecules from the nanorod surface. Moreover, further removal of the desorbed CTAB leads to the aggregation of the gold nanorods. Although efforts have been undertake to overcome this problem (Wang et al., 2006; Huang et al., 2009a; Pastoriza-Santos et al., 2006), new methods are preferred to directly prepare gold nanorods or analogous nanostructures without any surfactants.

On the other hand, when the gold nanostructures are used in the form of a liquid solution, the distributing signals from the changes of nanoparticle concentration are hard to be avoided (Huang et al., 2009b). Therefore, gold nanostructure films immobilized on transparent substrates have been employed extensively as potential transducers for LSPR sensing in the transmission mode (Huang et al., 2009b; Shon et al., 2009). Organic adhesion layers of amine- or mercapto-terminated silanes were commonly used in immobilization step. This may make their surfaces somewhat more inaccessible for functionalization with specific receptors or ligands. Therefore, a simple and effective scheme for the preparation of stable and "clean" gold nanostructure films on transparent solid substrate is to be desired.

Recently, Miller and Lazarides theoretically predicted that for any gold nanoparticles of moderate size in a homogeneous dielectric environment, the refractive index sensitivity is a function of only the LSPR band position, and independent of particle shape, size or composition (Miller and Lazarides, 2005). That is, for the same LSPR band location, the same refractive index sensitivity will be obtained for all arbitrarily shaped nanoparticles in a homogeneous dielectric environment. This provides an additional degree of freedom in preparing materials with desired properties and can allow combinations of properties not attainable with conventional materials. It is known that the LSPR of the small aggregated clusters would cause a new red-shifted plasmon adsorption attributed to the coupling of the plasmon absorbance of the adjacent particles (Yang et al., 2007; Basu et al., 2008; Matsubara et al., 2008). In this paper, we propose a novel low-cost electrochemical approach to controllable aggregation of twined-link gold naoparticles (TGNPs) with "clean" surface without introducing any template or surfactant. The TGNPs presented two LSPR bands, which is similar to that of gold nanorods. The as-prepared TGNPs on indium tin oxide (ITO) coated glass have very "clean" surface, which will make them to be easily functionalized. The preparation was found to have the desirable feature of technological simplicity and the resulted label-free LSPR biosensors were with the expected nature of sensitivity in sensing the antibody and antigen binding events.

2. Experimental and methods

2.1. Reagents and materials

ITO glass (1.1 mm thickness, 100 Ω) was purchased from Suzhou NSG Electronics Co., Ltd. (Suzhou, PR China). Mouse-immunoglobulin G (m-IgG), goat anti-mouse-immunoglobulin G (anti-m-IgG), and bovine serum albumin (BSA) were commercially obtained from Chengwen Biotechnology (Beijing, PR China). Hydrogen tetrachloroaurate ($HAuCl_4$) was products of Guoyao Chemical Regent Co., Ltd. The buffer solution (pH 2.0) was prepared by Na_2HPO_4 and citric acid. All other chemicals were analytical grade. Twice-distilled water was used throughout the experiments.

2.2. Electrochemical deposition of TGNPs on ITO glass surface

The TGNPs were prepared by electrochemical deposition on cyclic voltammetric mode. Briefly, the ITO glass was washed with NH_3–H_2O (1:20), ethanol, and distilled water for 10 min consequently in an ultrasonic bath. Then, it was immersed into the electrolyte which contained 0.1 mM $HAuCl_4$ and 0.1 M KCl in buffer solution (pH 2.0). Cyclic voltammogram was performed in quiescent solution which was deaerated by nitrogen gas for at least 10 min and a nitrogen atmosphere was kept over the solutions during the electrodeposition experiments. The electrolysis was kept at 60 °C. The parameters of cyclic voltammograms were the potential range from 0.3 V to −0.7 V for 20 cycles at a potential scan rate 0.05 V/s.

For comparison, the isolated gold nanoparticles (IGNPs) with about 60 nm diameter were also electrodeposited on ITO glass surface by the similar process. The composition of electrolyte was 0.2 mM $HAuCl_4$ in the buffer solution (pH 2.0). The chemical deposition was carried out in the potential range from 0.3 V to −0.6 V for 30 cycles at a scan rate 0.05 V/s in 30 °C water bath.

2.3. Immobilization of goat anti-m-IgG onto TGNPs/ITO surface

The TGNPs on ITO glass were functionalized as follows: the obtained TGNPs/ITO substrates were placed in a phosphate buffer solution (PBS, pH 7.4) containing 100 μg/mL goat anti-m-IgG and incubated for 12 h at 4 °C. The substrates were rinsed thoroughly with PBS.

2.4. Binding of m-IgG to goat anti-m-IgG functionalized TGNPs/ITO films

The glass substrates immobilized with goat anti-m-IgG were immersed in m-IgG solutions with different concentrations of m-IgG (1, 3, 5, 10, 100 and 500 ng/mL m-IgG in PBS buffer) for 3 h at 4 °C and rinsed thrice with PBS (pH 7.4).

2.5. Instrumentation

The electrodeposition experiments were performed on a CHI830B electrochemical workstation (Shanghai Chenhua Apparatus Corporation, China) in conjunction with a conventional three-electrode system. The working electrode was an ITO sheet, a platinum wire and a saturated calomel electrode served as the auxiliary and reference electrodes respectively. All the adsorption spectra were measured using a TU-1810 spectrophotometer (Beijing purkinje general instrument Co., Ltd., China). The various samples were measured against bare an ITO glass as a reference. Scanning electron microscopy (SEM) was obtained by using an S-4700 scanning electron microanalyzer (Hitachi, Japan) at an acceleration voltage of 15 kV. X-ray diffraction (XRD) analysis was carried out by X'Pert-Pro MPD (Panalytical, Holland).

3. Results and discussion

3.1. Characteristics of the TGNPs deposited on ITO glass surface

Electrochemical deposition of metal nanoparticles on a solid substrate involves two basic processes: nucleation and particle growth (Roustom et al., 2005). The size, density and distribution

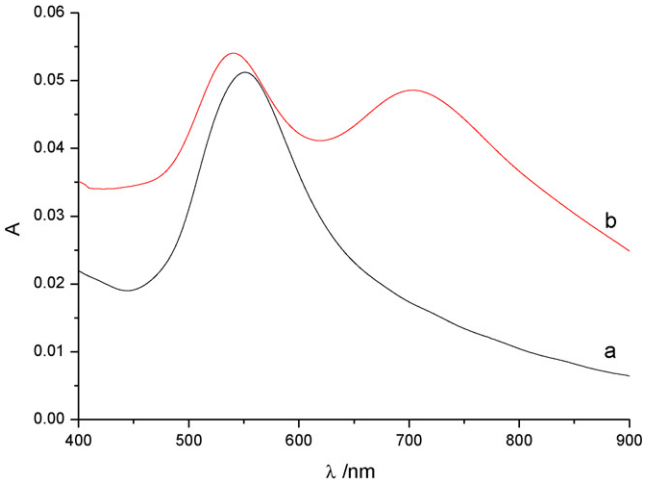

Fig. 1. UV–vis absorption spectra of IGNPs (a) and TGNPs (b) electrodeposited on ITO surface.

of particles depend largely on the competition between nucleation and growth. Fig. 1 shows the typical UV–vis absorption spectra of the IGNPs and TGNPs electrodeposited on ITO electrode surface at different electrolytic conditions. One single peak around 550 nm (Fig. 1a) represents the LSPR for isolated nanoparticles, which is ascribed to the collective oscillation of the free conduction band electrons of the particles. However, two peaks appear in the UV–vis absorption spectrum under controlling electrolytic conditions (Fig. 1b). Except for a peak about 540 nm, the second absorption band appears on the red side of the spectrum, indicating the occurrence of aggregation. This phenomenon is consistent with the previous reports (Basu et al., 2008, 2007a; Wang and Sun, 2006; Yang et al., 2007; Matsubara et al., 2008). Such an aggregation is ascribed to the linkage of adjacent gold nanoparticles. The former short wavelength is described to the transverse LSPR band of the GNP chains. The latter long wavelength is associated with the longitudinal mode of the electronic plasma oscillation along the long axis of the GNP chains. This is similar to the LSPR bands of gold nanorods.

In order to elucidate the electrochemical process, cyclic voltammograms for a 0.1 mM $HAuCl_4$ electrolyte solution were investigated (Figure S1). The first scan contains a characteristic "nucleation loop" which arises from the greater overpotential required for nucleation onto ITO surface compared to deposition of gold onto gold (Sheridan et al., 2007). The cathodic peak potential for the first scan is approximately 0.02 V while the peak potential for the subsequent scans is approximately 0.26 V. It is also suggests that the stripping process is incomplete in the first anodic process, that gold nuclei remain on the ITO surface and that subsequent growth occurs predominantly at the remaining gold sites rather than onto bare ITO surface. There is a single LSPR band at about 535 nm at deposition temperature 25 °C (Figure S2), which is consistent with our previous reports (Wang et al., 2009). However, two LSPR bands appear when the electrodeposition temperature arises to 60 °C. The latter peak comes from the aggregation of gold nanoparticles. Figure S3 shows the UV–vis spectra of gold nanoparticles fabricated by different deposition cycles. It can be seen that only one single peak around 525 nm existed at the electrodeposition 5 cycles. With increasing the electrodeposition cycles, the second absorption band appeared and increased. Especially, the peak was red-shifted gradually for the deposition from 10 to 20 cycles. From these experiments, it is demonstrated that the nucleation occur easily at high temperature and the nucleation process is also occur in subsequent potential scan. This suggests that the nucleation and particles growth take place simultaneously and lead to formation of aggregation at high deposition temperature. This results in the formation of aggregation of gold nanostructures. By carefully controlling the electrolysis conditions, the aggregation of GNPs on ITO electrode surface was controllable.

The morphology of as-prepared products was characterized by scanning electron microscopy (Fig. 2). Fig. 2a shows that the GNPs were deposited on ITO surface with a quite symmetric distribution. The average size of isolated gold nanoparticles was approximately 60 nm. However, from the SEM image (Fig. 2b), it is evident that gold nanoparticles are found to grow with chainlike aggregation. The average connection number of gold nanoparticles is about 2.3. This result is consistent with that of UV–vis absorption spectrum.

X-ray diffraction (XRD) was performed to study the crystalline nature of the gold nanoparticles on ITO surface (Fig. 3). The XRD pattern of the TGNPs is similar to that of isolated GNPs. An overwhelmingly intensive diffraction peak centered at $2\theta = 38.2^\circ$ was recorded, which corresponds to the (1 1 1) facet of the fcc crystal structure of gold (Rashid et al., 2007; Basu et al., 2007b). In contrast, the intensities of the peaks at $2\theta = 44.3$, 64.7, and 77.6° corresponding to (2 0 0), (2 2 0) and (3 1 1) lattice planes are quite weak.

3.2. Sensitivity of GNPs immobilized on ITO substrate to the refractive index variation of the surrounding media

In order to evaluate the sensitivity of LSPR for GNPs and TGNPs immobilized on ITO surface, the UV–vis absorption spectra were recorded from 400 to 1000 nm. 3 mL of individual solvent was taken out in a quartz cuvette whose inner wall was inserted an as-prepared glass, and the UV–vis adsorption spectrum was recorded

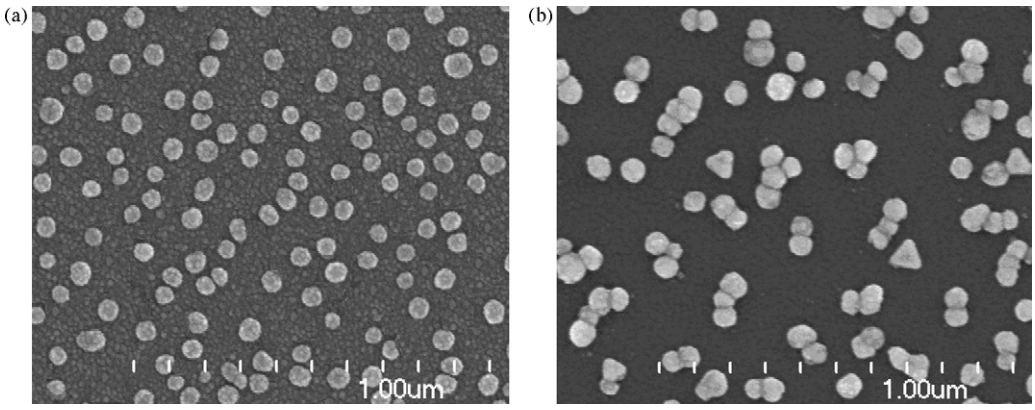

Fig. 2. Representative SEM images of IGNPs (a) and TGNPs (b) on ITO surface.

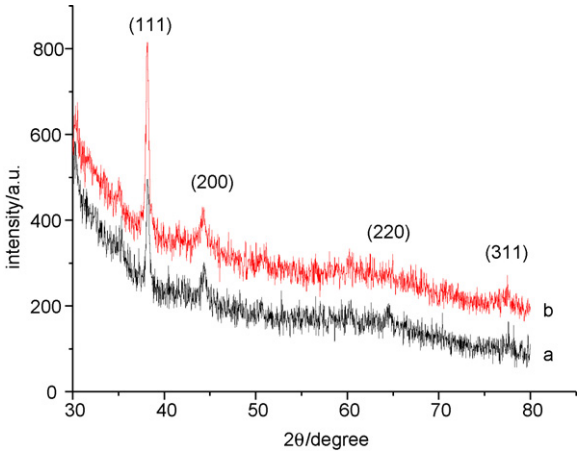

Fig. 3. XRD patterns of IGNPs (a) and TGNPs (b) electrodeposited on ITO surface.

against the bare ITO glass as a reference. Note that the cuvette and GNPs/ITO glass were washed completely and then dried every time, after each measurement of spectrum in the presence of a solvent. Fig. 4A shows the UV–vis absorption spectra of TGNPs immobilized on ITO glass immersed in various solvents. They are water, ether, acetone, ethanol, hexane, cyclohexane, benzene, carbon tetrachloride, trichloromethane and carbon disulfide, respectively. Fig. 4B plots the value of λ_{max} shift (λ_{max}(solvent) − λ_{max}(air)) of the LSPR for each GNPs-modified substrate as a function of the refractive index (RI) of the surround medium. Within this range of the RI, the data points for different peak can be fitted reasonably well to a straight line. Interpretation for this optical property changes is made on the basis of the Mie theory (Haes and Van Duyne, 2004; Stewart et al., 2008). The LSPR band maximum of GNPs is dependent on the dielectric constant of the surrounding medium in which the particles are embedded/dispersed. The index sensitivity of isolated GNPs-modified ITO glass is 78 nm/RIU. The index sensitivity of the TGNPs for the transverse surface plasmon wavelength of 540 nm is 65 nm/RIU and that of the longitudinal surface plasmon wavelength of 705 nm is 245 nm/RIU. The refractive index sensitivity of the TGNPs based on the longitudinal LSPR band is significantly higher than that of the Au nanospheres (76.4 nm/RIU) (Nath and Chilkoti, 2002), and similar to that of gold nanorods at about 700 nm band (252 nm/RIU) (Marinakos et al., 2007), but lower than that of the gold nanorods for the mean aspect ratio equal to 5.2 (366 nm/RIU) (Chen et al., 2007). Our results strongly suggest that the longitudinal LSPR wavelength of TGNPs is expected to be high sensitive to the interfacial binding events from biomolecular sensing, which is consistent with that of the gold nanorods. Therefore, the longitudinal LSPR band was used in all subsequent measurements for receptor-analyte binding.

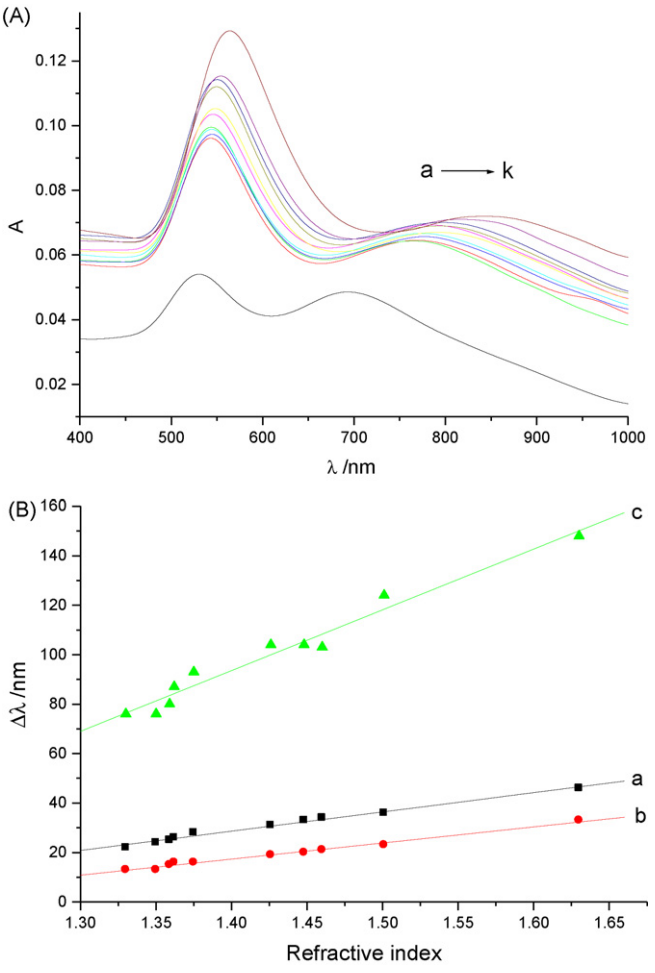

Fig. 4. (A) UV–vis absorption spectra TGNPs in different solvent. (a) Air; (b) water; (c) ether; (d) acetone; (e) ethanol; (f) hexane; (g) cyclohexane; (h) benzene; (i) carbon tetrachloride; (j) trichloromethane; (k) carbon disulfide. (B) Dependence of the λ_{max} shift on the refractive index for LSPR of IGNPs (a), transverse (b) and longitudinal (c) LSPR of TGNPs.

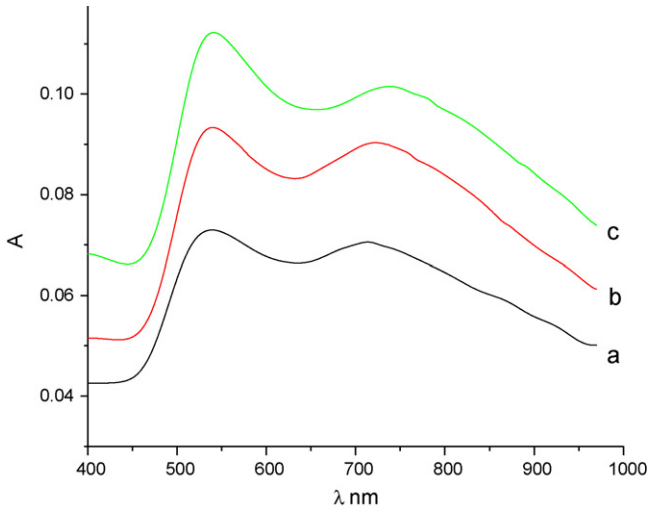

Fig. 5. UV–vis absorption spectra of TGNPs film immobilized on ITO substrate (a), TGNPs film after immobilization of goat anti-m-IgG (b), and the TGNPs film immobilized with goat anti-m-IgG after treatment with m-IgG in PBS buffer (c).

3.3. *Response of the longitudinal LSPR band at anti-m-IgG/TGNPs/ITO to the variation of m-IgG concentrations*

In order to demonstrate that the λ_{max} of the longitudinal LSPR band possesses detectable spectral responses for the biomolecular probe/target sensing events, we used the goat anti-m-IgG/m-IgG pair as a biosensing model compounds in this study. Our biosensing experiments were performed by the use of the anti-m-IgG/TGNPs/ITO as a probe. The goat anti-m-IgG immobilized onto TGNPs/ITO surface was performed by immersing the films in a solution of 100 μg/mL goat anti-m-IgG in PBS (pH 7.4) for 12 h at 4 °C. Their absorption spectra are shown in Fig. 5a and b. The longitudinal LSPR bands increased in intensity and were red-shifted 9 nm in wavelength, which is explained by the immobilization of goat anti-m-IgG onto the TGNPs/ITO surface. Subsequently, the TGNPs/ITO films functionalized by goat anti-m-IgG were immersed in solutions containing different concentration of m-IgG (1, 3, 5, 10, 100

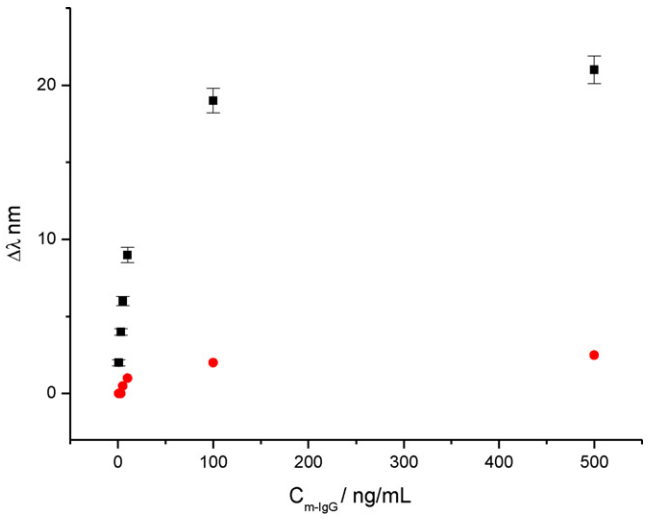

Fig. 6. The relationship between the concentrations of m-IgG and the shift of maximum transverse (●) and longitudinal (■) LSPR bands of TGNPs immobilized with goat anti-m-IgG. $N = 3$ for longitudinal LSPR band, $\Delta\lambda \pm$ SD.

and 500 ng/mL m-IgG in PBS) for 3 h. The LSPR band was red-shifted up to 21 nm and increased in intensity after the protein-recognition event (Fig. 5c). In addition, it is apparent that the change of Longitudinal LSPR band is much more than that of transverse LSPR band. For comparison, the LSPR band for the isolated GNPs immobilized with goat anti-m-IgG was red-shifted approximately 5 nm after incubated in 500 ng/mL m-IgG solution. Fig. 6 shows the resulting calibration curve of the determination for m-IgG. The longitudinal peak band increased with the increment of m-IgG concentration and became saturated at concentrations larger than 100 ng/mL m-IgG. Results showed that the use of the peak maximum of the longitudinal LSPR band in response to the concentration of the target molecules is sensitive, which is similar to the goat anti-human IgG biofunctionalization of silica-coated gold nanorods for detection of human-IgG (Wang et al., 2006). This suggests that the amount of m-IgG bioconjugated with goat anti-m-IgG/TGNPs/ITO was enhanced with increasing the concentration of m-IgG, films. With the m-IgG binding to goat anti-m-IgG attached on TGNPs, the refractive index in the vicinity of TGNPs will change, as a result, the adsorption intensity increases and maximum wavelength turns red-shift in response to a change in the refractive index. These results demonstrated that the surrounding medium influence both the plasmon frequency and the amplitude of the absorption. It also indicates that the molecular recognition of goat anti-m-IgG and m-IgG can be detected by changes in the longitudinal LSPR peak. The disadvantage is that the longitudinal peaks of the TGNPs are also more flat due to the variation of particle size and connection number. This may influence the peak defined features. Therefore, it is necessary to rigorously control the electrodeposition process.

In order to address the non-specific adsorption of other proteins on the TGNPs/ITO substrate after immobilization of goat anti-m-IgG, control experiment has been performed by adding 1 μg/mL bovine serum albumin instead of m-IgG. The LSPR band for the functionalization of TGNPs/ITO glass was almost no change after the incubation (Figure S4). This suggests that the changes in the absorption bands of the TGNPs/ITO films arise from specific goat anti-m-IgG and m-IgG binding. These experiments clearly show the potential of this sensing method for real biosensor applications.

4. Conclusions

We have developed a simple low-cost electrochemical route to fabricate twin-linked gold nanostructures with “clean” surface. The TGNPs films have been successfully used for fabrication of label-free m-IgG biosensors. The LSPR properties of TGNPs are similar to that of gold nanorods. This technique represents a simple and very straightforward method for making transparent substrates deposited with twin-linked gold nanostructures. More importantly, such TGNPs preserve not only the desirable feature of high refractive index sensitivity but also “clean” surface for further functionalization, which is critical for the preparation of stable and sensitive biosensors. Furthermore, this novel approach is promising as a simple and low-cost alternative to conventional biosensing techniques.

Acknowledgements

This work was supported by the National Natural Science Foundation of China (No. 20675055), the Science Foundations of the Education Bureau of Jiangsu Province (07KJB150101) and pre-research project of Soochow University.

Appendix A. Supplementary data

Supplementary data associated with this article can be found, in the online version, at doi:10.1016/j.bios.2010.07.014.

References

Basu, S., Pande, S., Jana, S., Bolisetty, S., Pal, T., 2008. Langmuir 24, 5562–5568.
Basu, S., Ghosh, S.K., Kundu, S., Panigrahi, S., Praharaj, S., Pande, S., Jana, S., Pal, T., 2007a. J. Colloid Interface Sci. 313, 724–734.
Basu, S., Praharaj, S., Pande, S., Jana, S., Pal, A., Ghosh, S.K., Pal, T., 2007b. J. Phys. Chem. C 111, 4596.
Beeram, S.R., Zamborini, F.P., 2009. J. Am. Chem. Soc. 131, 11689–11691.
Chen, C., Cheng, S., Chau, L., Wang, C.R.C., 2007. Biosens. Bioelectron. 22, 926–932.
Connor, E.E., Mwamuka, J., Gole, A., Murphy, C.J., Wyat, M.D., 2005. Small 1, 325–327.
Haes, A.J., Van Duyne, R.P., 2004. Anal. Bioanal. Chem. 379, 920–930.
Huang, H., Huang, S., Liu, X., Zeng, Y., Yu, X., Liao, B., Chen, Y., 2009a. Biosens. Bioelectron. 24, 3025–3029.
Huang, H., He, C., Zeng, Y., Xia, X., Yu, X., Yi, P., Chen, Z., 2009b. Biosens. Bioelectron. 24, 2255–2259.
Huang, X., Neretina, S., El-Sayed, M.A., 2009c. Adv. Mater. 21, 4880–4910.
Marinakos, S.M., Chen, S., Chilkoti, A., 2007. Anal. Chem. 79, 5278–5283.
Matsubara, S., Hayakawa, T., Yang, Y., Nogami, M., Okamoto, S., Koshikawa, N., 2008. J. Phys. Chem. C 112, 13917–13921.
Miller, M.M., Lazarides, A.A., 2005. J. Phys. Chem. B 109, 21556–21565.
Nath, N., Chilkoti, A., 2002. Anal. Chem. 74, 504–509.
Nath, N., Chilkoti, A., 2004. Anal. Chem. 76, 5370–5378.
Pastoriza-Santos, I., Pérez-Juste, J., Liz-Marzán, L.M., 2006. Chem. Mater. 18, 2465–2467.
Pérez-Juste, J., Pastoriza-Santos, I., Liz-Marzán, L.M., Mulvaney, P., 2005. Coord. Chem. Rev. 249, 1870–1901.
Rashid, M.H., Bhattacharjee, R.R., Mandal, T.K., 2007. J. Phys. Chem. C 111, 9684.
Roustom, B.E., Fóti, G., Comninellis, C., 2005. Electrochem. Commun. 7, 398–405.
Sepúlveda, B., Angelomé, P.C., Lechuga, L.M., Liz-Marzán, L.M., 2009. Nano Today 4, 244–251.
Sheridan, E., Hjelm, J., Forster, R.J., 2007. J. Electroanal. Chem. 608, 1–7.
Shon, Y., Choi, H.Y., Guerrero, M.S., Kwon, C., 2009. Plasmonics 4, 95–105.
Stewart, M.E., Anderton, C.R., Thompson, L.B., Maria, J., Gray, S.K., Rogers, J.A., Nuzzo, R.G., 2008. Chem. Rev. 108, 494–521.
Wang, C., Ma, Z., Wang, T., Su, Z., 2006. Adv. Funct. Mater. 16, 1673–1678.
Wang, G., Sun, W., 2006. J. Phys. Chem. B 110, 20901–20905.
Wang, Y., Deng, J., Di, J., Tu, Y., 2009. Electrochem. Commun. 11, 1034–1037.
Wang, Z., Ma, L., 2009. Coord. Chem. Rev. 253, 1607–1618.
Yang, D., Cui, D., 2008. Chem. Asian J. 3, 2010–2022.
Yang, Y., Matsubara, S., Nogami, M., Shi, J., 2007. Mater. Sci. Eng. B 140, 172–176.